An Unconditionally Stable Explicit Finite Difference Method for a Non-Dimensional Mathematical Model of Shoreline Evolution with a Twin Groins Structure

Surasak Manilam, and Nopparat Pochai

***Abstract*—The development of a more effective model and the prediction of trends in shorelines were the two goals of this study. For simulations of shoreline evolution utilizing the straight twin groin structure, we used two mathematical models. A one-dimensional evolution model makes up the initial model. The first model is transformed into a non-dimensional evolution model in the second model. We propose a method for transforming one-dimensional models into non-dimensional models, that involves creating initial and boundary conditions for each model. The forward time centered space (FTCS) technique and the Saulyev finite difference technique were applied to approximately represent shoreline evolution each year. Their simulation results demonstrate that when the engineering structure was built on the nearby shorelines, shoreline evolution accelerated annually. As the Saulyev finite difference technique is not restricted by the stability conditions, it produces better simulations.**

***Index Terms*— finite difference method, mathematical model, non-dimension model, shoreline evolution, twin-groin structure**

I. INTRODUCTION

THE issue of coastal erosion is a natural process that changes the shoreline's physical qualities. The processes of wind, waves, currents, changes in sea level, and the imbalance of sand sediment all have an influence on there. The shoreline models require being analyzed and qualitatively evaluated in order to predict future topographic changes.

Mathematical models are used to solve a wide variety of problems in both science and engineering. For example, the problems of transportation pollution [1], [2], salinity in rivers, streams, and groundwater [3], [4], and the distribution of contaminants in the waking lake [5], [6]. These problems can be explained by the diffusion equations. The most popular coastline transformation model has seven models: 1) ONELINE model (One-line Model), 2) GENESIS model (Generalized model for simulating shoreline change), 3) LITPACK model (Littoral processes and coastline kinetics) [7], 4) UNIBEST model (Uniform beach sediment transport), 5) GENCADE model (Genesis and cascade), 6) SMC model (Sistema de modelado costero) [8], and 7) BEACHPLAN model. Each model is suitable for sandy or pebbly beaches and subject to different limitations associated with its use. In [9], they describe the development of a coastal morphological model. Recommended for the full and time-based simulation of the evolution of the coastline in which the coastline is governed by practical and reliable structures and boundary conditions. Additionally, the capabilities of the ONELINE model were tested by comparing the results with actual measured data. In [10], they introduced a numerical modeling region called GENESIS, which is used to model long-term coastal changes caused by spatial and temporal changes. The objective of the research [11] was to determine the optimal values for the coefficients K1 and K2 so that the predicted coastal changes had an acceptable correlation with the results of satellite data processing. The results showed that the predictions were well correlated with the data and the numerical models. GENESIS was applicable not only for coastal predictions on sandy beaches but also for muddy beaches. In [12], they describe the hypothesis and the development of governing equations in a general form. In addition, they present a technique used to obtain more than 25 analytical solutions, which cover situations related to both structured and unstructured shoreline change. For example, beach filling of initial shape, sand mining, river discharge, groin and jetty and breakwater etc. In [13], they describe an extension of the concept for analytical solutions of existing single-line models taking into account arbitrary time-varying wave conditions. In addition, it gives an initial shoreline shape an arbitrary function of coastline distance which in practice can be determined by survey. An explicit solution is obtained from the technique of integral transformation. This new semi-analytical solution has a more complex expression form than the previous analytical expression obtained from steady-state waves. The general expression of the semi-analytical solution can be used to describe time-varying wave conditions for the initial beach shape as a function of arbitrary position and for the source of sediment as a known function that depends on time and space. But these solutions are extremely effective and have a

Manuscript received May 27, 2023; revised November 20, 2023.

This work was supported by the Centre of Excellence in Mathematics, the Ministry of Higher Education, Science, Research and Innovation, Bangkok, Thailand.

Surasak Manilam is a PhD candidate of Mathematics Department, School of Science, King Mongkut's Institute of Technology Ladkrabang, Bangkok, 10520, Thailand (e-mail: surasak.manilam915@gmail.com).

Nopparat Pochai is an associate professor of Mathematics Department, School of Science, King Mongkut's Institute of Technology Ladkrabang, Bangkok, 10520, Thailand (corresponding author to provide phone: 662329-8400; fax: 662-329-8400; e-mail: nop_math@yahoo.com).

few errors. Moreover, the new solution provides a valuable tool to extend the range of solutions by which it can test the accuracy and convergence of time-dependent finite-difference numerical models.

In [14], they introduced a one-dimensional model of shoreline evolution with two or three groin structures. They have also extended the concept by taking the wavelength influence on the structure into account in the system. In research [15], they introduced a governing model called a non-dimensional model. This model was used to simulate the change in coastlines when a single groin was built and used to manipulate physical parameters. It is useful in terms of computational time and reduced budget. Moreover, they also introduced an unconditionally stable explicit numerical technique to estimate the model's solution.

In this research, we have two objectives: the first is to study the model's effectiveness. We developed the model to achieve higher efficiency and faster computation time by converting it to a non-dimensional model. Thus, there are two governing models: one-dimensional and non-dimensional shoreline evolution models. The last is to predict the trend in long-term erosion and deposition along shores where the twin groins are constructed. Moreover, we also introduced the determination of initial and boundary conditions suitable for the model. The finite difference techniques are used to approximate the model's solution.

II. A Shoreline Evolution Model

A. *The Governing Equation*

A fundamental mathematical model for describing coastal change was developed under the conservation of sand volume and two primary assumptions:

1) The beach profile retains the average shape of the coastline. Although, it is constantly moving seaward and shoreward. For all points on this profile, it is enough to determine the location of the entire profile with respect to a baseline. So, one contour-line can used to describe the change in the shape and volume of a beach plan. In addition, we use this contour-line to identify it easier to the coastline;

2) The profile moves within two well-defined limiting heights i.e., the berm height D_B and the depth of closure D_C. Both heights were measured from the vertical datum, this is the mean sea-level (MSL), etc.

Thus, we obtain the following differential equation for shoreline evolution:

$$\frac{\partial y}{\partial t} = \frac{1}{D_B + D_C}\left(-\frac{\partial Q}{\partial x}\right) , \qquad (1)$$

where y is the cross-shore position of shoreline (m), x is the longshore distance (m), t is time (day), D_C is the depth of closure (m), D_B is the berm height (m), and Q is the longshore transport rate (m^3/day). The model state variable is the position of the shoreline $y(x,t)$, which is a function of time t and coordinate x.

The longshore sand transport rate is the quantity created by a wave that strikes the coastline obliquely. The coastal engineering research center [16] has recommended the general term for longshore sand transport rates Q as follows:

$$Q = Q_0 \sin\left(2\alpha_b\right) , \qquad (2)$$

where Q_0 is the amplitude of the long-shore sand transport rate, and α_b is the impact angle between breaking wave crests angle with local shoreline. The quantity Q_0 is derived empirically, it is expressed as a functional relationship with parameters in which can written as [17]:

$$Q_0 = \frac{\rho}{16}\left(H_b^2 c_{bg}\right)\frac{K}{\left(\rho_s - \rho\right)\left(1-n\right)} , \qquad (3)$$

where the subscript b represent the value at the point breaking, ρ is the density of sea water (kg/m^3), ρ_s is the density of the sediment (kg/m^3), n is the porosity, K is the dimensionless coefficient which is a function of particle size, H is the wave height (m), and c_g is the wave group velocity (m/day). Equation (3) is called the empirical predictive formula for the amplitude of the long-shore sand transport rate.

The impact angle between breaking wave crests angle with local shoreline α_b can be written as:

$$\alpha_b = \alpha_0 - \tan^{-1}\left(\frac{\partial y}{\partial x}\right) , \qquad (4)$$

where α_0 is the angle between breaking wave crests and the x-axis (degree). For a beach with a slight slope, the angle of incidence that the breaking waves make against the shoreline is negligible. Therefore, it is assumed that

$$\sin\left(2\alpha_b\right) \approx 2\alpha_b , \qquad (5)$$

and

$$\tan^{-1}\left(\frac{\partial y}{\partial x}\right) \approx \left(\frac{dy}{dx}\right) . \qquad (6)$$

Substituting (4) into (2), and using the assumptions for the angle of incidence (5)-(6), we obtain (7) as follows:

$$Q = Q_0\left(2\alpha_0 - 2\frac{\partial y}{\partial x}\right) . \qquad (7)$$

Substituting (7) into (1), we obtain (8) as follows:

$$\frac{\partial y}{\partial t} = D\frac{\partial^2 y}{\partial x^2} , \qquad (8)$$

for all $(x,t) \in \Omega$ such that $\Omega = [0,L]\times[0,\tau]$, $\tau = 360t_Y$, $L > 0$, $\tau > 0$, where t_Y is time (years), L is the distance of shoreline (m) and

$$D = \frac{2Q_0}{D_B + D_C} . \qquad (9)$$

Equation (8) is a parabolic partial differential equation, so we have to define initial and boundary conditions under this problem. The coefficient D is a coefficient describing the time scale of the shoreline change after wave action. Therefore, a high amplitude of long-shore sand transport rate Q_0 will enable rapid shoreline responses. On the other hand, a large depth of closure D_C will slow the response of the coastline. The concept of shoreline evolution with a straight twin groin structure is illustrated in Figs. 1-2 below.

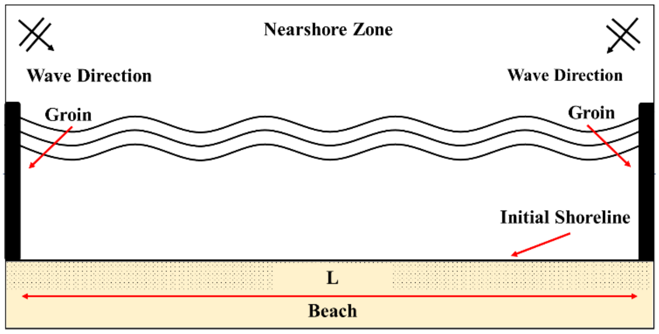

Fig. 1. The shoreline begins with a straight twin groin structure.

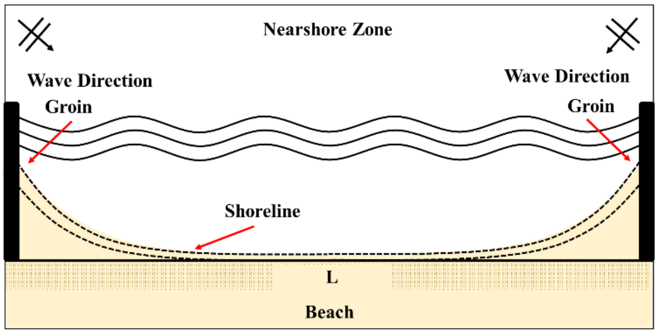

Fig. 2. Shoreline evolution with a straight twin groin structure.

B. The Initial and Boundary Conditions of the One-Dimensional Model

Suppose that the initial shoreline contour is in equilibrium where it is parallel to the x-axis and that every location has the same wave incidence angle. Therefore, the expression of the initial condition is

$$y(x,0)=0 \ , \tag{10}$$

for all $x \in [0,L]$. The expressions of left and right boundary conditions are defined as follows:

$$\frac{\partial y}{\partial x} = \tan(-\alpha_0) \ \text{at} \ x=0 \ , \tag{11}$$

$$\frac{\partial y}{\partial x} = \tan(\alpha_0) \ \text{at} \ x=L \ , \tag{12}$$

for all $t \in [0,\tau]$.

Both of these expressions can be used to immediately indicate the position of shorelines on groins when structures are used to block the transport of sand. The above setting conditions are illustrated in Figs. 3-4.

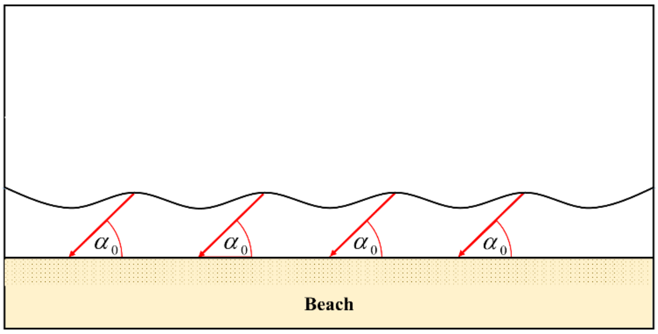

Fig. 3. Breaking wave crests impact angle (the version is redrawn based on [15]).

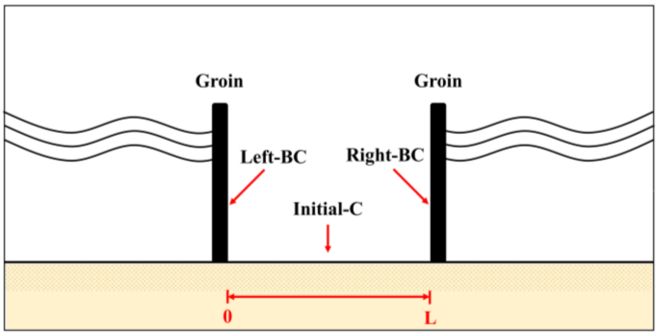

Fig. 4. Setting initial and boundary conditions.

III. A Non-Dimensional Model

A. The Non-Dimensional Shoreline Evolution Model

Applying the dimensionless technique [18] to (8), where the variables $X = x/L$ and $Y = y/Y_*$ are defined as the non-dimensional variables and applying the chain rules of

$$\frac{\partial y}{\partial x} = \frac{\partial y}{\partial X}\left(\frac{1}{L}\right) , \tag{13}$$

$$\frac{\partial y^2}{\partial x^2} = \frac{1}{L^2}\frac{\partial^2 y}{\partial X^2} . \tag{14}$$

We obtain

$$\frac{\partial Y}{\partial t} = \frac{D}{L^2}\frac{\partial^2 Y}{\partial X^2} . \tag{15}$$

Dividing by the coefficient of the highest order derivative term and setting $T = Dt/L^2$ or $t = L^2T/D$. Then we substitute t on the left-hand side of (15), we obtain the following non-dimensional shoreline evolution equation:

$$\frac{\partial Y}{\partial T} = \frac{\partial^2 Y}{\partial X^2} , \tag{16}$$

for all $(X,T) \in \Psi$ such that $\Psi = [0,1]\times[0,\eta]$, $\eta = \dfrac{D\tau}{L^2}$ and $\eta > 0$, where Y_* is the expected evolution (m),

$$Y = \frac{y}{Y_*} , \tag{17}$$

$$X = \frac{x}{L} , \tag{18}$$

$$T = \frac{Dt}{L^2} . \tag{19}$$

B. The Initial and Boundary Conditions of the Non-Dimensional Model

In order for all the conditions of both models to be corresponding, we apply dimensionless technique [18] to those conditions in (10)-(12). The initial condition becomes

$$Y(X,0)=0 . \tag{20}$$

The left and right boundary conditions become

$$\frac{\partial Y}{\partial X}=\frac{L}{Y_*}\tan\left(-\alpha_0\right) \text{ at } X=0 , \tag{21}$$

and

$$\frac{\partial Y}{\partial X}=\frac{L}{Y_*}\tan\left(\alpha_0\right) \text{ at } X=1 . \tag{22}$$

IV. NUMERICAL TECHNIQUES

In this section, we begin by considering dividing the domains Ψ into the mesh-grids, where we divide the closed interval [0,1] into M sub-intervals and the closed interval $\left[0,\eta\right]$ into N sub-intervals, which means that $M\Delta X=1$ and $N\Delta T=\eta$ respectively. Any point on the grid $\left(X_m,T_n\right)$ is defined by $X_m=m\Delta X$ and $T_n=n\Delta T$ for all indices $m=0,1,\ldots,M$ and $n=0,1,\ldots,N$, in which both M and N are non-negative integers, ΔX and ΔT are the X-axis and the T-axis increments (step size). Therefore, we can substitute the approximation at any point on the grid by $Y\left(X_m,T_n\right)$, or we can write it using the notation Y_m^n. The solutions of the model in section III are numerically approximated using the forward time centered space (FTCS) techniques and the Saulyev finite difference (Saulyev) technique.

A. The Forward Time Centered Space (FTCS) Technique

Applying the forward time centered space (FTCS) technique [19] to (16). We have the following finite difference approximation [15]:

$$Y\left(X_m,T_n\right)\cong Y_m^n , \tag{23}$$

$$\frac{\partial Y}{\partial T}\cong\frac{Y_m^{n+1}-Y_m^n}{\Delta T} , \tag{24}$$

$$\frac{\partial Y}{\partial X}\cong\frac{Y_{m+1}^n-Y_{m-1}^n}{2\,\Delta X} , \tag{25}$$

$$\frac{\partial^2 Y}{\partial X^2}\cong\frac{Y_{m+1}^n-2Y_m^n+Y_{m-1}^n}{\Delta X} . \tag{26}$$

Substituting (23)-(26) into (16), we obtain the following finite difference equation:

$$\frac{Y_m^{n+1}-Y_m^n}{\Delta T}=\frac{Y_{m+1}^n-2Y_m^n-Y_{m-1}^n}{\left(\Delta X\right)^2} . \tag{27}$$

The equation (27) can be arranged in the explicit finite difference form as follows:

$$Y_m^{n+1}=\mu Y_{m+1}^n+\left(1-2\mu\right)Y_m^n+\mu Y_{m-1}^n , \tag{28}$$

where $m=1,2,\ldots,M-1$, $n=0,1,\ldots,N-1$ and $\mu=\frac{\Delta T}{\left(\Delta X\right)^2}$.

B. The Saulyev Finite Difference (Saulyev) Technique

Applying the Saulyev finite difference technique [20] to (16). We have the following finite difference approximation [21]:

$$Y\left(X_m,T_n\right)\cong Y_m^n , \tag{29}$$

$$\frac{\partial Y}{\partial T}\cong\frac{Y_m^{n+1}-Y_m^n}{\Delta T} , \tag{30}$$

$$\frac{\partial Y}{\partial X}\cong\frac{Y_{m+1}^n-Y_{m-1}^n}{2\,\Delta X} , \tag{31}$$

$$\frac{\partial^2 Y}{\partial X^2}\cong\frac{Y_{m+1}^n-Y_m^n-Y_m^{n+1}+Y_{m-1}^{n+1}}{\left(\Delta X\right)^2} . \tag{32}$$

Substituting (29)-(32) into (16), we obtain the following finite difference equation:

$$\frac{Y_m^{n+1}-Y_m^n}{\Delta T}=\frac{Y_{m+1}^n-Y_m^n-Y_m^{n+1}+Y_{m-1}^{n+1}}{\left(\Delta X\right)^2} . \tag{33}$$

The equation (33) can be arranged in the explicit finite difference form as follows:

$$Y_m^{n+1}=\left(1+\mu\right)^{-1}\left[\mu Y_{m+1}^n+\left(1-\mu\right)Y_m^n+\mu Y_{m-1}^{n+1}\right] , \tag{34}$$

where $m=1,2,\ldots,M-1$, $n=0,1,\ldots,N-1$ and $\mu=\frac{\Delta T}{\left(\Delta X\right)^2}$.

C. The Application of the Traditional Forward Time Centered Space (FTCS) Technique to the Left and Right Boundary Conditions

In this problem, we have a Neumann left and right boundary condition. At the left boundary and right boundary points on the domain, we cannot approximate using (28) and (34) because those equations generate points outside of the domain. Those points are called the fictitious points. We approximated the solution by applying the forward time centered space (FTCS) technique [19] to (16). We have the following finite difference approximation:

$$Y\left(X_m,T_n\right)\cong Y_m^n , \tag{35}$$

$$\frac{\partial Y}{\partial T}\cong\frac{Y_m^{n+1}-Y_m^n}{\Delta T} , \tag{36}$$

$$\frac{\partial Y}{\partial X}\cong\frac{Y_{m+1}^n-Y_{m-1}^n}{2\,\Delta X} , \tag{37}$$

$$\frac{\partial^2 Y}{\partial X^2}\cong\frac{Y_{m+1}^n-2Y_m^n+Y_{m-1}^n}{\Delta X} . \tag{38}$$

Substituting (35)-(38) into (16) and rearranging it in the explicit finite difference form as follows:

$$Y_m^{n+1}=\mu Y_{m+1}^n+\left(1-2\mu\right)Y_m^n+\mu Y_{m-1}^n , \tag{39}$$

for all $m=1,2,\ldots,M-1$, $n=0,1,\ldots,N-1$ and

$$\mu = \frac{\Delta T}{(\Delta X)^2}, \ \omega = \frac{2L(\Delta X)}{Y_*}.$$

For $m = 0$, we eliminate the fictitious point Y_{-1}^n using the central finite difference technique with the Neumann left boundary condition. We obtain the approximation at the fictitious point:

$$Y_{-1}^n = Y_1^n - \omega \tan(-\alpha_0) . \quad (40)$$

Substituting (40) into (39) and rearranging it in the explicit finite difference form as follows:

$$Y_m^{n+1} = 2\mu Y_{m+1}^n + (1-2\mu) Y_m^n - \omega\mu \tan(-\alpha_0) . \quad (41)$$

For $m = M$, we eliminate the fictitious point Y_{M+1}^n using the central finite difference technique with the Neumann right boundary condition. We obtain the approximation at the fictitious point:

$$Y_{M+1}^n = Y_M^n - \omega \tan(\alpha_0) . \quad (42)$$

Substituting (42) into (39) and rearranging it in the explicit finite difference form as follows:

$$Y_m^{n+1} = (1-2\mu) Y_m^n + 2\mu Y_{m-1}^n + \omega\mu \tan(\alpha_0) . \quad (43)$$

Equations (41) and (43) can be used to find approximate solutions on the left boundary and right boundary points on the domain.

V. NUMERICAL EXPERIMENT AND RESULT

Consider the shoreline evolution occurring between a straight twin groin structure as shown in Figs. 1-2. Let y be the position of the shoreline (m). The distance between the structures is $L = 600$ m. The expected evolution over 1-25 years is $Y_* = 60$ m.

The sediment density is $\rho_s = 1700$ kg/m^3. The sea water is $\rho = 1020$ kg/m^3. The porosity is $n = 0.406$. The non-dimensional coefficient of particle size is $K = 0.375$. The averaged berm height is $D_B = 2$ m. The averaged closure depth is $D_C = 28$ m. The relevant physical parameters are listed in Table I below.

TABLE I
PARAMETERS

Meaning	Symbol (Unit)	Values
The sediment density	$\rho_s \ (kg/m^3)$	1700
The sea water	$\rho \ (kg/m^3)$	1020
The porosity	n	0.406
The non-dimensional coefficient which is a function of particle size	K	0.375
The averaged berm height	$D_B \ (m)$	2
The averaged closure depth	$D_C \ (m)$	28

Field data of the wave group velocity and the wave height for each month over a year measured in the Gulf of Thailand [14] are shown in Table II below.

TABLE II
THE WAVE GROUP VELOCITY AND THE WAVE HEIGHT

Month	$c_g \ (m/day)$	$H \ (m)$
January	8951.04	1.5
February	6998.40	1.5
March	5866.56	0.5
April	6920.64	1.5
May	5719.68	0.5
June	5546.88	0.5
July	8225.28	1.5
August	1246.07	1.5
September	1825.95	1.5
October	5580.26	2.5
November	1448.57	1.5
December	1517.60	1.5

The amplitudes of the long-shore sand transport rate are calculated by (3) and they are listed in Table III and Fig. 5 below.

TABLE III
THE AMPLITUDE OF THE LONG-SHORE SAND TRANSPORT RATE

Month	$Q_0 \ (m/day)$
January	1191.99
February	931.96
March	86.80
April	921.61
May	84.63
June	82.07
July	1095.34
August	1246.07
September	1825.95
October	5580.26
November	1448.57
December	1515.60
Average	**1334.40**

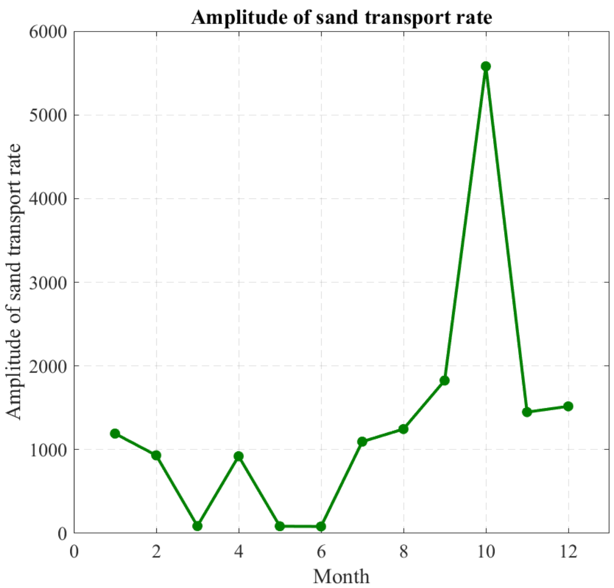

Fig. 5. Amplitude of the long-shore sand transport rate.

In our assumption, we assume that the amplitudes of the long-shore sand transport rate are equal every year, so their average is $Q_0 = 1334.40$ m/day. The angle impact of the breaking wave is $\alpha_0 = 0.02$ (degree). The T-axis increment is $\Delta T = 0.0002471 \ (N = 9000)$. The X-axis increment is $\Delta X = 0.0416667 \ (M = 24)$. We will approximate the solution of (16) under the constraints corresponding to the initial and boundary conditions (20)-(22) by using two numerical techniques: the forward time centered space (FTCS) and the Saulyev finite difference (Saulyev) techniques. For the internal points of the domain, we use (28) and (34), respectively. As for the remaining points of the domain (left and right boundary), we use (41) and (43), respectively. Since we now have a dimensionless solution. To convert our solutions to one-dimensional solutions, we can easily find them by using the relation of the variables (17)-(19): $y = YY_*$, $x = XL$, and $t = L^2 D^{-1} T$.

TABLE IV
COMPARISON OF THE STABILITY OF EACH TECHNIQUE WHEN CHANGING THE GRID SIZES.

Δx	ΔX	Δt	ΔT	Stability	
				FTCS	**Saulyev**
		1	0.0002	S	S
		5	0.0012	U	S
25	0.0417	10	0.0025	U	S
		15	0.0037	U	S
		30	0.0074	U	S
		1	0.0002	S	S
		5	0.0012	S	S
50	0.0833	10	0.0025	S	S
		15	0.0037	U	S
		30	0.0074	U	S
		1	0.0002	S	S
		5	0.0012	S	S
100	0.1667	10	0.0025	S	S
		15	0.0037	S	S
		30	0.0074	S	S
		1	0.0002	S	S
		5	0.0012	S	S
150	0.2500	10	0.0025	S	S
		15	0.0037	S	S
		30	0.0074	S	S
		1	0.0002	S	S
		5	0.0012	S	S
200	0.3333	10	0.0025	S	S
		15	0.0037	S	S
		30	0.0074	S	S
		1	0.0002	S	S
		5	0.0012	S	S
300	0.5000	10	0.0025	S	S
		15	0.0037	S	S
		30	0.0074	S	S

Note: U := Unstable and S := Stable

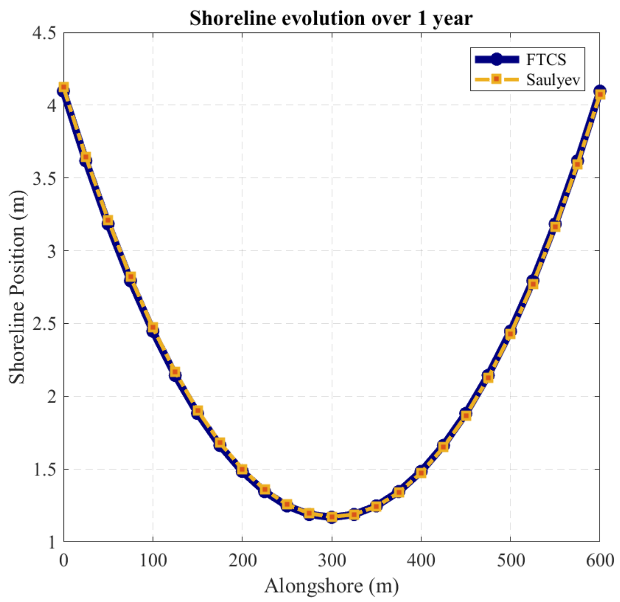

Fig. 6. The approximated shoreline evolution over 1 year.

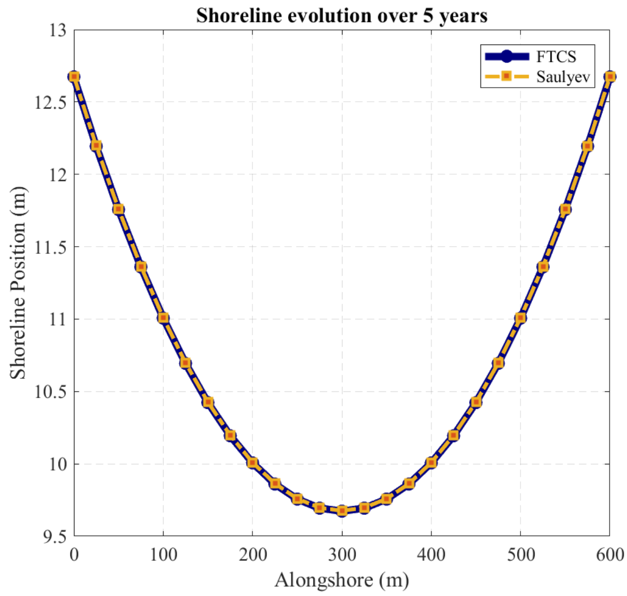

Fig. 7. The approximated shoreline evolution over 5 years.

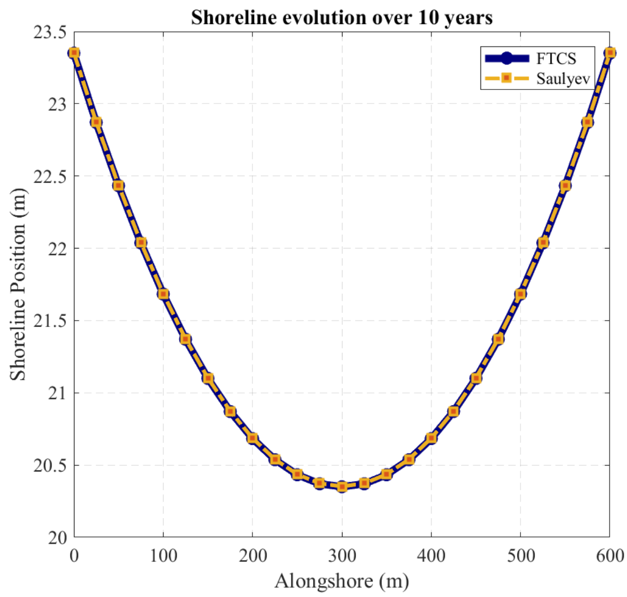

Fig. 8. The approximated shoreline evolution over 10 years.

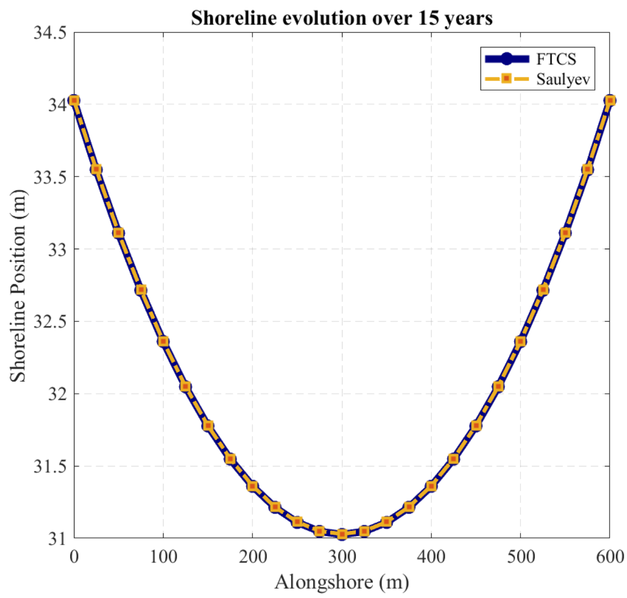

Fig. 9. The approximated shoreline evolution over 15 years.

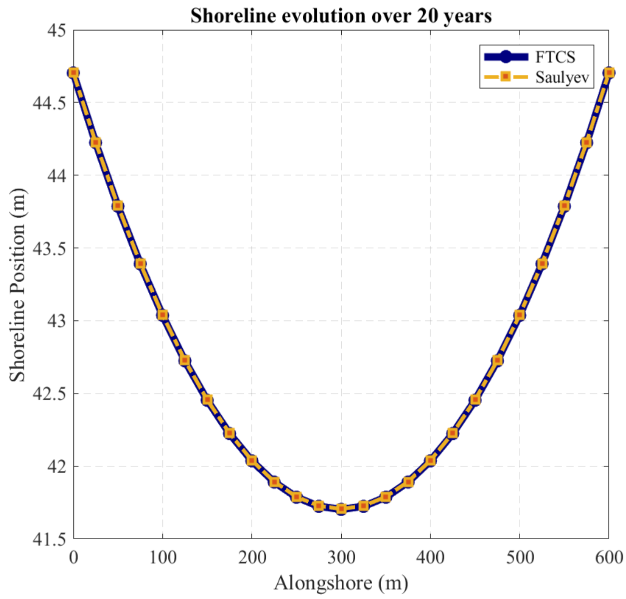

Fig. 10. The approximated shoreline evolution over 20 years.

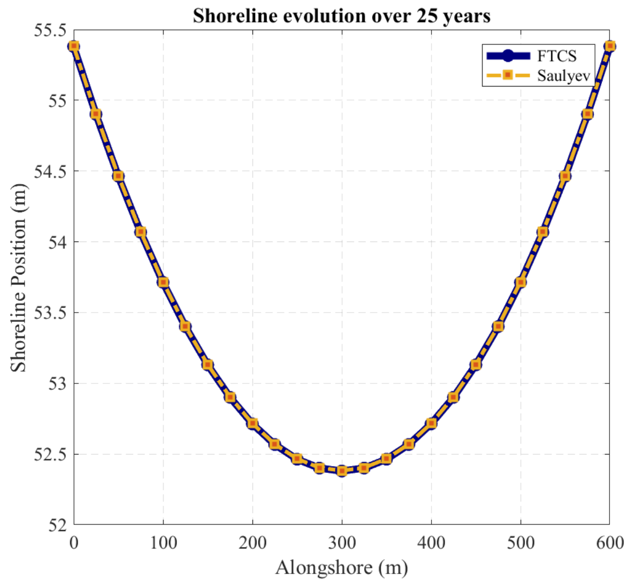

Fig. 11. The approximated shoreline evolution over 25 years.

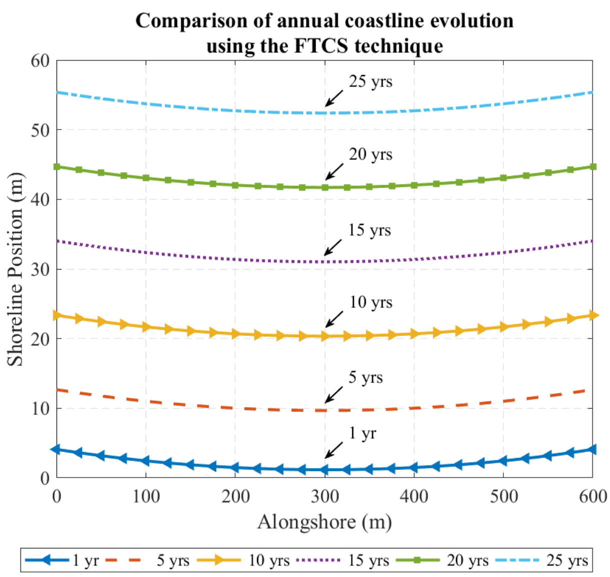

Fig. 12. Comparison of annual shoreline evolution approximated using the FTCS technique.

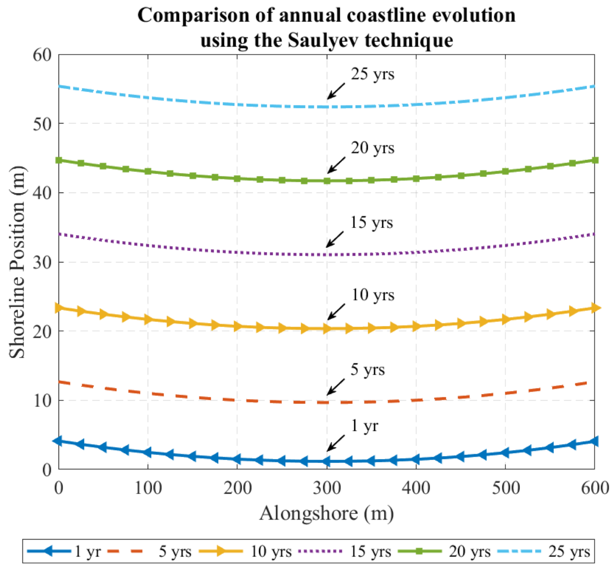

Fig. 13. Comparison of annual shoreline evolution approximated using the Saulyev technique.

The value of approximated shoreline evolution, which uses the forward time centered space (FTCS) and the Saulyev finite difference (Saulyev) techniques, are listed in Tables V-VI. The absolute and the total-absolute differences between the two techniques for each year are listed in Table VII.

TABLE V
THE APPROXIMATED SHORELINE EVOLUTION OVER 20 YEARS USING THE FORWARD TIME CENTERED SPACE (FTCS) TECHNIQUE.

Time (Years)	Distances (m) 0	50	100	150	200
0	0.0000	0.0000	0.0000	0.0000	0.0000
1	4.0955	3.1836	2.4469	1.8818	1.4834
5	12.6734	11.7567	11.0066	10.4231	10.0064
10	23.3501	22.4333	21.6832	21.0998	20.6831
15	34.0267	33.1100	32.3599	31.7764	31.3597
20	44.7034	43.7866	43.0365	42.4531	42.0364
25	55.3800	54.4633	53.7132	53.1297	52.7130

Time (Years)	Distances (m) 250	300	350	400	450
0	0.0000	0.0000	0.0000	0.0000	0.0000
1	1.2468	1.1683	1.2468	1.4834	1.8818
5	9.7564	9.6730	9.7564	10.0064	10.4231
10	20.4330	20.3497	20.4330	20.6831	21.0998
15	31.1097	31.0263	31.1097	31.3597	31.7764
20	41.7863	41.7030	41.7863	42.0364	42.4531
25	52.4630	52.3796	52.4630	52.7130	53.1297

Time (Years)	Distances (m) 500	550	600
0	0.0000	0.0000	0.0000
1	2.4469	3.1836	4.0955
5	11.0066	11.7567	12.6734
10	21.6832	22.4333	23.3501
15	32.3599	33.1100	34.0267
20	43.0365	43.7866	44.7034
25	53.7132	54.4633	55.3800

VI. Discussion

The measurements of shoreline position (shoreline evolution) can be simulated into dimensional and non-dimensional mathematical models. In which both models can be defined parameters that correspond to reality are not different.

TABLE VI
THE APPROXIMATED SHORELINE EVOLUTION OVER 20 YEARS USING THE SAULYEV FINITE DIFFERENCE (SAULYEV) TECHNIQUE TECHNIQUE.

Time (Years)	Distances (m)				
	0	50	100	150	200
0	0.0000	0.0000	0.0000	0.0000	0.0000
1	4.1233	3.2108	2.4721	1.9034	1.5000
5	12.6771	11.7603	11.0101	10.4266	10.0097
10	23.3529	22.4362	21.6861	21.1026	20.6859
15	34.0296	33.1128	32.3627	31.7793	31.3626
20	44.7062	43.7895	43.0394	42.4559	42.0392
25	55.3829	54.4661	53.7160	53.1326	52.7159
Time (Years)	250	300	350	400	450
0	0.0000	0.0000	0.0000	0.0000	0.0000
1	1.2572	1.1718	1.2432	1.4734	1.8665
5	9.7594	9.6759	9.7590	10.0089	10.4254
10	20.4359	20.3525	20.4359	20.6859	21.1026
15	31.1125	31.0292	31.1125	31.3626	31.7793
20	41.7892	41.7058	41.7892	42.0392	42.4559
25	52.4658	52.3825	52.4658	52.7159	53.1326
Time (Years)	500	550	600		
0	0.0000	0.0000	0.0000		
1	2.4277	3.1621	4.0733		
5	11.0087	11.7587	12.6755		
10	21.6860	22.4361	23.3529		
15	32.3627	33.1128	34.0296		
20	43.0394	43.7895	44.7062		
25	53.7160	54.4661	55.3829		

TABLE VII
THE ABSOLUTE DIFFERENCE BETWEEN BOTH NUMERICAL TECHNIQUES.

Time (Years)	Distances (m)				
	0	50	100	150	200
0	0.0000	0.0000	0.0000	0.0000	0.0000
1	0.0278	0.0271	0.0251	0.0216	0.0166
5	0.0037	0.0036	0.0036	0.0034	0.0033
10	0.0029	0.0029	0.0029	0.0028	0.0028
15	0.0028	0.0028	0.0028	0.0028	0.0028
20	0.0028	0.0028	0.0028	0.0028	0.0028
25	0.0028	0.0028	0.0028	0.0028	0.0028
Time (Years)	250	300	350	400	450
0	0.0000	0.0000	0.0000	0.0000	0.0000
1	0.0104	0.0035	0.0035	0.0100	0.0154
5	0.0031	0.0028	0.0026	0.0024	0.0023
10	0.0028	0.0028	0.0028	0.0028	0.0028
15	0.0028	0.0028	0.0028	0.0028	0.0028
20	0.0028	0.0028	0.0028	0.0028	0.0028
25	0.0028	0.0028	0.0028	0.0028	0.0028
Time (Years)	500	550	600	Total	
0	0.0000	0.0000	0.0000	0.0000	
1	0.0193	0.0215	0.0222	0.2241	
5	0.0021	0.0021	0.0020	0.0371	
10	0.0028	0.0028	0.0028	0.0369	
15	0.0028	0.0028	0.0028	0.0369	
20	0.0028	0.0028	0.0028	0.0369	
25	0.0028	0.0028	0.0028	0.0369	

Two numerical techniques, namely the forward time centered space (FTCS) and the Saulyev finite difference (Saulyev) techniques were used. The results are listed in Tables V-VI, respectively.

For the FTCS and Saulyev techniques after 1 year as illustrated in Fig. 6, the highest shoreline position was 4.0955 and 4.1233 m, respectively, and the lowest shoreline position was 1.1638 and 1.1718 m, respectively.

For the FTCS and Saulyev techniques after 5 years as illustrated in Fig. 7, the highest shoreline position was 12.6734 and 12.6771 m, respectively, and the lowest shoreline position was 9.6730 and 9.6759 m, respectively.

For the FTCS and Saulyev techniques after 10 years as illustrated in Fig. 8, the highest shoreline position was 23.3501 and 23.3529 m, respectively, and the lowest shoreline position was 20.3497 and 20.3525 m, respectively.

For the FTCS and Saulyev techniques after 15 years as illustrated in Fig. 9, the highest shoreline position was 34.0267 and 34.0296 m, respectively, and the lowest shoreline position was 31.0263 and 31.0292 m, respectively.

For the FTCS and Saulyev techniques after 20 years as illustrated in Fig. 10, the highest shoreline position was 44.7034 and 44.7062 m, respectively, and the lowest shoreline position was 41.7030 and 41.7058 m, respectively.

For the FTCS and Saulyev techniques after 25 years as illustrated in Fig. 11, the highest shoreline position was 55.3800 and 55.3829 m, respectively, and the lowest shoreline position was 52.3796 and 52.3825 m, respectively.

As in Fig. 12-13, if we compare each year, it will be found that shoreline evolution tends to increase continuously. In addition, we also found that the results obtained from the two numerical techniques were close as listed in Table VII. Therefore, there was no difference in choosing from either of these two techniques. But if the stability conditions ($0 < \mu < 0.5$) are taken into account, the Saulyev technique may be a better choice since it is not constrained by the stability conditions as listed in Table IV.

VII. CONCLUSION

We demonstrate how the shoreline changes as a straight twin-groin construction is constructed. A one-dimensional model and a non-dimensional model, both of which may evaluate local shoreline lengths and physical parameters, make up the proposed shoreline evolution model. Here, we also describe a process for transforming a one-dimensional model into a non-dimensional model, which includes initial and boundary conditions. The forward time-centered space (FTCS) and Saulyev finite difference techniques were employed for the numerical approximation method. The results of the modeling show the following: 1) The shoreline evolution accelerated annually when the engineering structure was constructed on the nearby shorelines; 2) Twin groins have a higher evolution efficiency than single groins; 3) The non-dimensional model provides great computational flexibility; 4) The Saulyev method is an unconditionally explicit finite difference method. Therefore, this method yields highly accurate calculation results and reduces the calculation time when large time increments are required. Therefore, this method yields highly accurate calculation results and reduces the calculation time when large time increments are required. The proposed computational techniques are able to be applied in several oceanic scenarios and other types of groins.

REFERENCES

[1] H. Huang, Y. Akutsu, M. Arai, and M. Tamura, "A Two-Dimensional Air Quality Model in an Urban Street Canyon: Evaluation and Sensitivity Analysis," *Atmospheric Environment*, vol. 34, no. 5, pp.689–698, 2000, doi: 10.1016/S1352-2310(99)00333-7.

[2] K. Suebyat, and N. Pochai, "Numerical Simulation for a Three-Dimensional Air Pollution Measurement Model in a Heavy Traffic Area Under the Bangkok Sky Train Platform," *Abstract and Applied Analysis*, vol. 2018, pp.1–10, 2018, doi: 10.1155/2018/9025851.

[3] P. Othata, and N. Pochai, "A One-Dimensional Mathematical

Simulation to Salinity Control in a River With a Barrage Dam Using an Unconditionally Stable Explicit Finite Difference Method," *Advances in Difference Equations*, vol. 2019, no. 1, 2019, doi: 10.1186/s13662-019-2106-4.

[4] S. Khatbanjong, and N. Pochai, "Numerical Groundwater Quality Assessment Model Using Two-Level Explicit Methods," *Engineering Letters*, vol. 29, no. 1, pp.183–190, 2021.

[5] I. Ghosh, M. S. H. Chowdhury, S. M. Aznam, and M. M. Rashid, "Measuring the Pollutants in a System of Three Interconnecting Lakes by the Semianalytical Method," *Journal of Applied Mathematics*, vol. 2021, no. 1, pp.1-16, 2021, doi: 10.1155/2021/6664307.

[6] N. Camcoon, and N. Pochai, "A Non-dimensional Mathematical Model of Salinity Measurement in the Chaophraya River Using a New Fourth Order Finite Difference Method With the Saulyev Technique," *Engineering Letters*, vol. 28, no. 4, pp.978–984, 2020.

[7] DHI Water & Environment, "Litpack: Noncohesive Sediment Transport in Currents and Waves," *DHI Water & Environment*. Denmark: Danish Hydraulic Institute: Horsholm, 2005.

[8] M. Gonzalez, R. Medina, J. Gonzalez-Ondina, A. Osorio, F. J. Mendez, and E. Garcia, "An Integrated Coastal Modeling System for Analyzing Beach Processes and Beach Restoration Projects, SMC," *Computers and Geosciences*, vol. 33, no. 7, pp.916–931, 2007, doi: 10.1016/j.cageo.2006.12.005.

[9] M. Dabees, and J. W. Kamphuis, "Oneline: a Numerical Model for Shoreline Change," *In Proceedings of the 26th International Conference on Coastal Engineering*, Denmark, 1998, pp.2668–2681, doi: 10.1061/9780784404119.202.

[10] H. Hanson, "Genesis-A Generalized Shoreline Change Numerical Model," *Journal of Coastal Research*, vol. 5, no. 1, pp.1–27, 1989.

[11] S. Sutikno, K. Murakami, D. P. Handoyo, and M. Fauzi, "Calibration of Numerical Model for Shoreline Change Prediction Using Satellite Imagery Data," *Makara Journal of Technology*, vol. 19, no. 3, pp.113-119, 2015, doi: 10.7454/mst.v19i3.3042.

[12] M. Larson, H. Hanson, and N. C. Kraus, "Analytical Solutions of the One-Line Model of Shoreline Change," *US Army Corps of Engineer Waterway Experiment Station, Coastal Engineering Research Center*, Washington, 1987.

[13] A. Zacharioudaki, and D. E. Reeve, "Semianalytical Solutions of Shoreline Response to Time-Varying Wave Conditions," *Journal of Waterway, Port, Coastal, and Ocean Engineering*, vol. 134, no. 5, pp.265–274, 2008, doi: 10.1061/(asce)0733-950x(2008)134:5(265).

[14] P. Unyapoti, and N. Pochai, "A Shoreline Evolution Model With a Twin Groins Structure Using Unconditionally Stable Explicit Finite Difference Techniques," *Engineering Letters*, vol. 29, no. 1, pp.288–296, 2021.

[15] S. Manilam, and N. Pochai, "A Non-dimensional Mathematical Model of Shoreline Evolution With a Groin Structure Using an Unconditionally Stable Explicit Finite Difference Technique," *IAENG International Journal of Applied Mathematics*, vol. 52, no. 2, pp.473-841, 2022.

[16] B. Le Mahaute, and M. Soldate, "Mathematical Modeling of Shoreline Evolution," *In Proceedings of the 16th Conference on Coastal Engineering*, Hamburg, 1978, pp.1163-1179, doi: 10.9753/icce.v16.67.

[17] M. M. Subiyanto, M. F. Ahmad, M. Mamat, and M. L. Husain, "Comparison of Numerical Method for Forward and Backward Time Centered Space for Long-Term Simulation of Shoreline Evolution," *Applied Mathematical Sciences*, vol. 7, no. 104, pp.5165–5173, 2013, doi: 10.12988/ams.2013.37365.

[18] G. D. Smith, *Numerical Solution of Partial Differential Equation: Finite Difference*. New York: Oxford University, 1985, ch. 2.

[19] S. C. Chapra, and R. P. Canale, *Numerical Methods for Engineers*. New York: McGraw-Hill, 2012, ch. 30.

[20] M. T. Darvishi, "Forward-Backward Saul'yev Methods to Solve PDEs," *WSEAS Transation on Mathematics*, vol. 2, no. 1, pp.1–5, 2003.

[21] B. F. Towler and R. Y. K. Yang, "Numerical Stability of the Classical and the Modified Saul'yev's Finite-Difference Methods," *Computers and Chemical Engineering*, vol. 2, no. 1, pp.45–51, 1978, doi: 10.1016/0098-1354(78)80006-4.